Triplet Correlations Dominate the Transition from Simple to Tetrahedral Liquids

Murari Singh,[1] Debdas Dhabal,[2] Andrew Huy Nguyen,[3] Valeria Molinero,[3] and Charusita Chakravarty[2,*]
[1]School of Physical Sciences, Jawaharlal Nehru University, New Delhi 110067, India
[2]Department of Chemistry, Indian Institute of Technology-Delhi, New Delhi 110016, India
[3]Department of Chemistry, The University of Utah, Salt Lake City, Utah 84112-0850, USA
(Received 10 August 2013; published 10 April 2014)

The total, triplet, and pair contributions to the entropy with increasing tetrahedrality are mapped out for the Stillinger-Weber liquids to demonstrate the qualitative and quantitative differences between triplet-dominated, tetrahedral liquids and pair-dominated, simple liquids with regard to supercooling and crystallization. The heat capacity anomaly of tetrahedral liquids originates in local ordering due to both pair and triplet correlations. The results suggest that structural correlations can be directly related to thermodynamic anomalies, phase changes, and self-assembly in other atomic and colloidal fluids.

DOI: 10.1103/PhysRevLett.112.147801 PACS numbers: 61.20.-p, 64.70.D-, 65.20.-w

The behavior of complex fluids, including the self-assembly processes underlying the formation of ordered structures, is strongly influenced by multiparticle correlations though the relationships between structural correlations and thermodynamics are not well understood [1–3]. In contrast, phase transformations and liquid-state behavior of simple fluids are dominated by pair correlations and are relatively well characterized. Here we address the changing relationships between structural correlations and thermodynamics that underlie the transformation of a simple liquid into a complex, tetrahedral liquid dominated by triplet correlations, driven by a systematic variation of the degree of anisotropy of the interparticle interactions. Tetrahedral fluids are among the simplest of complex fluids and include a number of important systems, such as water, ionic melts (SiO_2,BeF_2), covalently bonded liquids (C, Si), metalloids (Ge, Sn), and dispersions of patchy colloids [4–13]. They show a density-driven shift from four-coordinate, local order at low densities to random, close-packing arrangements at high densities. Depending on the degree of energetic preference for local tetrahedral order, they display several differences in comparison to simple liquids, including density and related response function anomalies, negative volume changes on melting, crystalline polymorphism, and polyamorphism [10,14–18]. Our motivation here is to understand the competition between pair and triplet correlations that underlies the transformation of a simple liquid into a complex, tetrahedral liquid, using the multiparticle correlation expansion for the entropy to translate the information on pair and triplet correlations into thermodynamic signatures associated with liquid state behavior and phase transformations [19–24]. As a model system, we use the Stillinger-Weber family of liquids that captures much of the complex phenomenology of tetrahedral liquids, especially with regard to water and silicon [5,15–18,25–30]. We show that as a function of tetrahedrality, the liquid state can be subdivided into pair- and triplet-dominated regimes, separated by a narrow, glass-forming region where orientational disorder within the first neighbor shell is significant. The three regimes show qualitatively different thermodynamic behavior on supercooling, with the low-tetrahedrality liquids conforming to the temperature scaling and melting rules expected of simple liquids, while the triplet-dominated systems show a characteristic heat capacity anomaly reflecting local ordering due to pair and triplet correlations prior to crystallization.

The total entropy of a monoatomic, homogeneous, and isotropic fluid can be written using the multiparticle correlation expansion as $S = S_{\rm id} + S_2 + S_3 + \ldots$, where S_n is the contribution due to the n-particle correlations [19–24,31,32]. $S_{\rm id}$ is the entropy of the ideal gas at the same temperature and density and is given in units of k_B per particle by $S_{\rm id} = 5/2 - \ln(\rho\Lambda^3)$, where ρ is the fluid density, Λ is the thermal de Broglie wavelength, k_B is the Boltzmann constant, and N is the number of particles. The pair entropy (S_2) per particle in units of k_B is defined by

$$S_2 = -2\pi\rho \int_0^\infty [g^{(2)}(r)\ln g^{(2)}(r) - g^{(2)}(r) + 1]r^2 dr, \quad (1)$$

where $g^{(2)}(r)$ is the radial distribution function as a function of the pair spacing r. The triplet correlation, $g^{(3)}(r,s,t)$, between three particles located at positions $\mathbf{r}_1$, $\mathbf{r}_2$, and $\mathbf{r}_3$ is written as a function of three relative distances, $r = |\mathbf{r}| = |\mathbf{r}_2 - \mathbf{r}_1|$, $s = |\mathbf{s}| = |\mathbf{r}_3 - \mathbf{r}_1|$, and $t = |\mathbf{s} - \mathbf{r}|$ [33–35]. The irreducible part of the triplet correlation function, $g^{(3)}(r,s,t)$ is

$$\delta g^{(3)}(r,s,t) = g^{(3)}(r,s,t)/[g^{(2)}(r)g^{(2)}(s)g^{(2)}(t)]. \quad (2)$$

The triplet entropy (S_3) per particle in units of k_B is

$$S_3 = -\frac{\rho^2}{6}\int\int g^{(3)}(r,s,t)\log[\delta g^{(3)}(r,s,t)]d\mathbf{r}d\mathbf{s} + \frac{\rho^2}{6}\int\int\Big\{g^{(3)}(r,s,t) - g^{(2)}(r)g^{(2)}(s) - g^{(2)}(s)g^{(2)}(t) - g^{(2)}(r)g^{(2)}(t) + g^{(2)}(r) + g^{(2)}(s) + g^{(2)}(t) - 1\Big\}d\mathbf{r}d\mathbf{s}. \quad (3)$$

The Stillinger-Weber (SW) interaction potential is the sum of an isotropic two-body (ϕ_2) and an anisotropic three-body (ϕ_3) term favoring local tetrahedral order, $U = \sum_{\text{pair}}\phi_2 + \lambda\sum_{\text{triplet}}\phi_3$, where the first and second terms represent sums over unique pairs and unique triplets, respectively. The pair potential is

$$\phi_2(r_{ij}) = A\epsilon\left[B\left(\frac{\sigma}{r_{ij}}\right)^4 - 1\right]\exp\left(\frac{\sigma}{r_{ij} - a\sigma}\right) \quad (4)$$

and the three-body interaction term is

$$\phi_3(r_{ij}, r_{ik}, \theta_{ijk}) = \epsilon(\cos\theta_{ijk} - \cos\theta_0)^2 \times \exp\left(\frac{\gamma\sigma}{r_{ij} - a\sigma}\right)\exp\left(\frac{\gamma\sigma}{r_{ik} - a\sigma}\right). \quad (5)$$

The parameter values were $A = 7.049556277$, $B = 0.6022245584$, $\gamma = 1.2$, $a = 1.8$, $\theta_0 = 109.47°$ with the tetrahedral parameter λ, varied over the range from 15 to 30. Several tetrahedral liquids can be modeled as SW fluids, such as silicon ($\lambda = 21$), germanium ($\lambda = 20$), tin ($\lambda = 18.5$), and water [$\lambda = 23.15$ or monoatomic water (mW) model] [5,15–18]. The simulations were performed using the mass $m = 18$ a.m.u., distance $\sigma = 2.3925$ Å and energy $\epsilon = 3116.0686$ K of the monatomic water model (mW). The LAMMPS simulation package was used for molecular dynamics simulations [18]. Computational details are given in the Supplemental Material [36]. Unless otherwise stated, all quantities are reported in reduced units based on the well depth (ϵ) and length scale (σ) parameters of the two-body term (ϕ_2).

The three-body term in the SW potential enhances three-body correlations relative to pair correlations and increases the magnitude of S_3 relative to S_2. In the tetrahedrality-temperature (λT) plane at a given pressure, the $S_2 = S_3$ curve separates pair-dominated liquids from triplet-dominated liquids. Figure 1 shows S_2 and S_3 as a function of λ at different temperatures; triplet-dominated behavior shifts to higher tetrahedralities with increasing temperature. We juxtapose the $S_2 = S_3$ curve for the stable liquid regime against the previously mapped out phase diagram and anomalous regimes at zero pressure [15,17,18]. The crystalline phases show sharp transitions from body-centered cubic (bcc) ($\lambda < 18$), to a β-tin structure near the pseudoeutectic ($\lambda = 18.75$) to a cubic diamond or tetrahedral structure ($\lambda > 18.75$). The density (ρ) anomaly, corresponding to a negative thermal expansion coefficient, is

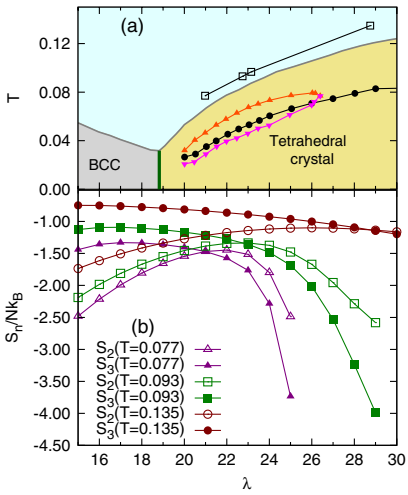

FIG. 1 (color online). (a) Phase diagram of the Stillinger-Weber liquids in the tetrahedrality-temperature ($\lambda - T$) plane at zero pressure. The locus of points at which $S_2 = S_3$ is shown with open squares. The locus of temperatures of maximum and minimum density are shown in red (Δ) and pink (∇), respectively. The line of heat capacity maxima is shown with black, filled circles. (b) Variation of S_2 and S_3 along isotherms with $T = 0.135$, 0.093, and 0.077. We exclude λ values for which convergence problems are observed at low temperatures [36].

observable in the intermediate tetrahedrality regime, $19 < \lambda < 26.5$. The heat capacity (C_p) anomaly corresponds to a sharp increase in heat capacity on isobaric cooling. The line representing the heat capacity anomaly corresponds to maxima in $C_p(T)$ obtained in fast cooling ramps, or, alternatively, the metastability limit of the liquid in longer, equilibrium runs. The locus of the heat capacity maxima lies approximately 30%–40% below the melting line of the tetrahedral crystal from $\lambda > 21.5$ to high tetrahedralities. The $S_2 = S_3$ curve runs approximately parallel to the melting line of the tetrahedral crystal, at a temperature approximately 15%–20% above the melting line. Pair-dominated SW liquids crystallize to form bcc structures, indicating the relatively soft, short-range pair repulsion [37]. The triplet-dominated liquids crystallize to form a tetrahedral, diamond structure while a narrow intermediate tetrahedrality regime ($18 < \lambda < 20$) tends to vitrify. The transformation of the liquid to a triplet-dominated fluid seems to strongly favor formation of a tetrahedral crystal, as well as the existence of a heat capacity anomaly.

For systems with specific degrees of tetrahedrality, Fig. 2 shows the triplet correlation functions, $g^{(3)}(r,r,s)$, for isosceles triangle configurations for which $s^2 = 2r^2(1 - \cos\theta)$. The pair-dominated $\lambda = 16$ system displays a strong peak at 60°, consistent with locally icosahedral configurations seen in simple liquids. Close to the eutectic ($\lambda = 18$), the orientational disorder within the first neighbor shell is striking with peaks at 60°, 75°, and 100°, and must be associated with the strong glass-forming propensities in this regime. Once the eutectic is crossed, even for a low tetrahedrality system like germanium with $\lambda = 20$, the

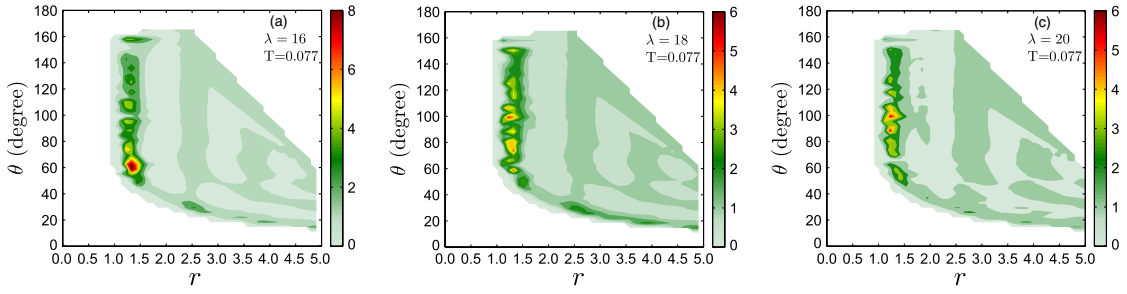

FIG. 2 (color online). Triplet correlation functions $g^{(3)}(r, r, s)$ for isosceles triangle configurations for SW liquids at $T = 0.077$ with tetrahedrality values of (a) $\lambda = 16$, (b) $\lambda = 18$, and (c) $\lambda = 20$. Contour plots have axes labeled by r (in units of σ) and θ, such that $s^2 = 2r^2 - 2r^2\cos(\theta)$ with the scale shown on the side. Zero values of $g^{(3)}$ are due to either excluded volume effects, boundary conditions, or the triangle inequality.

orientational preference within the first neighbor shell is clearly centered at $\theta = 109.5°$. The formation of a second neighbor shell at about 1.8σ is notable and becomes more pronounced with increasing tetrahedrality, as does the orientational preference for the tetrahedral angle. The triplet correlation functions therefore highlight three qualitatively distinct regimes of local structural order and associated crystallization behavior: (i) pair-dominated liquids crystallizing into bcc structures; (ii) a narrow eutectic regime with significant first neighbor-shell disorder and strong glass-forming propensities, and (iii) a triplet-dominated regime which crystallizes into a tetrahedral lattice.

We now compare the temperature-dependent behavior of liquids on the low- and high-tetrahedrality sides of the eutectic, using the $\lambda = 16$ and $\lambda = 23.15$ systems as representative examples. The $\lambda = 23.15$ system is the well-studied monoatomic water (mW) model [17,25–27,29,30,38,39]. Each system is cooled isobarically from a relatively high temperature to the lower limit of liquid state stability when homogeneous nucleation takes place. The total entropy (S) of the fluid is determined by Widom insertion at a relatively high temperature, followed by thermodynamic integration along an isobar [36]. The thermodynamic excess entropy at a state point (T, P, ρ) along the isobar is defined relative to the ideal gas at the same temperature (T) and density (ρ). Convergence of pair and triplet entropies with respect to simulation length, and the bin width and range associated with integration has been checked. Since error bars for entropic quantities cannot be directly estimated, in keeping with earlier studies [22,23,32], we show convergence with integration range and estimate that the errors in S_2 and S_3 are less than $0.05k_B$ [36]. Figure 3 compares S_e, S_2, and S_3 for the $\lambda = 16$ and $\lambda = 23.15$ liquids along the $P = 3.2269 \times 10^{-5}$ isobar. Figure 4 compares the total isobaric heat capacity, $C_p = T(\partial S/\partial T)_P$ with the pair, $C_2 = T(\partial S_2/\partial T)_P$, and triplet, $C_3 = T(\partial S_3/\partial T)_P$, contributions. A useful correction to the pair entropy was derived earlier for state points where compressibility is low and $\delta g^{(n)}$ for $n > 2$ is close to unity [32]. We derive an analogous expression, $S_e \approx S_2 + S_3 - (1/3)$, and test its accuracy along the $P = 3.2269 \times 10^{-5}$ isobar for the $\lambda = 16$ and $\lambda = 23.15$ systems. The numerical values of various entropic quantities, along with the thermal expansion coefficient (α) and the isothermal compressibility (κ_T) are tabulated in the Supplemental Material [36].

We first consider isobaric cooling of the pair-dominated $\lambda = 16$ SW liquid. Density functional theory for inverse power law fluids predicts a $T^{-2/5}$ temperature dependence of S_e, as well as a value of $S_e \approx -4k_B$ at freezing [40,41]. The $\lambda = 16$ liquid satisfies the $T^{-2/5}$ scaling over the temperature range from $T = 0.18$ to $T_{\rm thr} = 0.035$, where $T_{\rm thr}$ represents the threshold temperature below which the liquid crystallizes during the simulation run [36]. The values of S_e at T_m and $T_{\rm thr}$ are $-4.7k_B$ and $-5.4k_B$, respectively, consistent with results for other simple liquids [3,42–46]. The total isobaric heat capacity, C_p, shows a small rise on supercooling from $3.5k_B$ to $4k_B$. There is no accompanying rise in compressibility or thermal expansivity, unlike in the case of tetrahedral liquids. We now consider the pair and triplet contributions to the fluid entropy. At high temperatures, the dominant contribution to S_e is from S_2 and $S_e \approx S_2 + S_3 - (1/3)$. Close to and

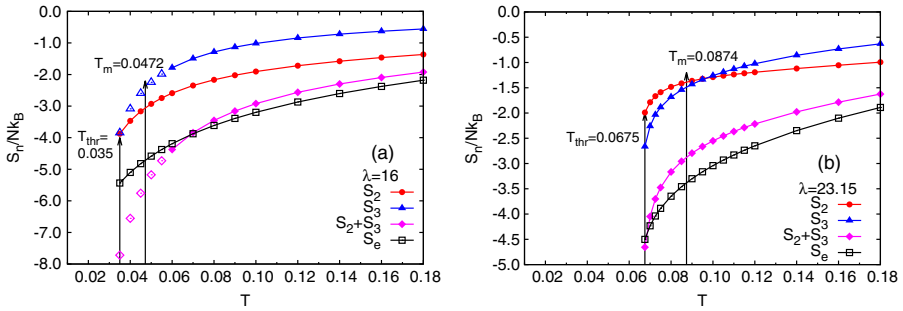

FIG. 3 (color online). The excess (S_e), pair (S_2), and triplet (S_3) entropies as a function of temperature (T) at $P = 1$ atm for (a) $\lambda = 16$ and (b) $\lambda = 23.15$. Data for state points at which S_3 does not converge within 5σ are shown with open, rather than filled, symbols.

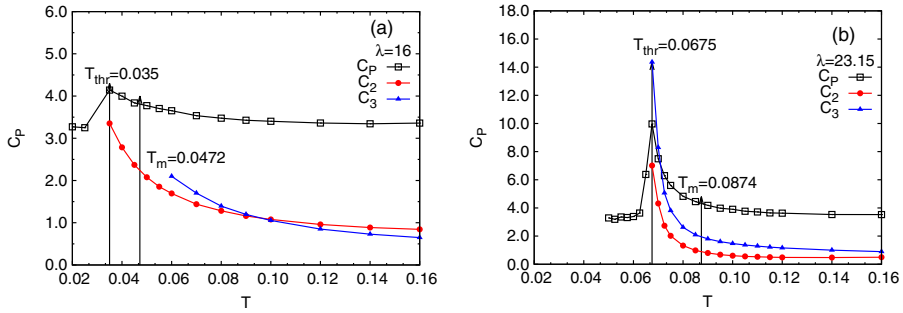

FIG. 4 (color online). The total (C_P), pair (C_2), and triplet (C_3) as a function of temperature (T) for (a) $\lambda = 16$ and (b) $\lambda = 23.15$.

below solid-liquid coexistence at T_m, this approximation breaks down and the convergence of S_3 with a range of integration slows down significantly due to long-range correlations in $\delta g^{(3)}$, resulting in an apparent steep decrease in S_3 on supercooling [36]. The long-range triplet correlations may reflect intermediate-range bond orientational ordering prior to crystallization, as suggested in recent studies of simple liquids [47]. We note that S_e itself does not show any steep decrease on supercooling, suggesting that the liquid as a whole must be strongly frustrated and S_n contributions for $n > 3$ must be positive at low temperatures.

The behavior of the triplet-dominated, $\lambda = 23.15$ (mW water) system contrasts significantly with the pair-dominated system [Figs. 3(b) and 4(b)]. The $T^{-2/5}$ scaling of S_e is seen only at high temperatures and the S_e values at T_m and T_{thr} do not conform to those seen for simple liquids. At high temperatures, the C_p values of the $\lambda = 16$ and $\lambda = 23.15$ systems are comparable. The anomalous rise in C_p on isobaric cooling is, however, very pronounced with a value of $5k_B$ at T_m and $10k_B$ at T_{thr}. The S_2 and S_3 contributions for the tetrahedral liquid are well converged for $0.0675 < T < 0.18$ and $S_2 + S_3 \geq S_e$, except close to T_{thr}. The sharp rise in $C_p(T)$ is closely tracked by $C_2(T)$ and $C_3(T)$. The approximation $S_e \approx S_2 + S_3 - (1/3)$ works fairly well for this system over the entire range of temperature studied, even close to the mestastability limit of the crystal. The reasons for this unexpected difference between tetrahedral and pair-dominated liquids requires further study, but we speculate that this may be because there is no difference in local order between the tetrahedral liquid and the corresponding crystal. To summarize, pair and triplet contributions to the entropy and heat capacity in tetrahedral liquids closely track the corresponding thermodynamic quantities, in contrast to the triplet contributions for pair-dominated liquids. The structural reorganization and the associated thermodynamic features (e.g., heat capacity anomaly) on supercooling of tetrahedral liquids is therefore qualitatively different from that seen in pair-dominated systems.

The locus of state points for which pair and triplet correlations to the entropy are equal serves to demarcate the liquid regime of the Stillinger-Weber systems into pair- and triplet-dominated regimes. Using the triplet correlation functions, we show that the nature of local order within the first neighbor shell is a critical factor in determining the behavior on supercooling. The pair- and triplet-dominated liquids crystallize into body-centered cubic and diamond structures, respectively, while a narrow range of intermediate tetrahedrality with strong disorder within the first neighbor shell is associated with strong, glass-forming propensities. The low-tetrahedrality liquids behave essentially as simple liquids in terms of the temperature dependence of the excess entropy, conformity to freezing rules, and a very weak rise in heat capacity on approaching the metastability limit of the liquid. The triplet-dominated liquids show a characteristic anomalous rise in heat capacity on isobaric cooling that can be attributed almost entirely to the collective reorganization of the liquid structure due to increasing strength of pair and triplet correlations. In contrast, the pair-dominated liquids show increasing long-range triplet correlations on approaching crystallization but no sharp rise in either the pair or thermodynamic heat capacities. Our study complements other recent work on supercooling and crystallization pathways of water and silicon, using the Stillinger-Weber as well as other atomistic models, in that we focus on the direct effect of structural correlations on calorimetric signatures of liquid-state behavior. We note that information on triplet correlations is potentially accessible from isobaric pressure derivatives of the structure factor [48]. Preliminary results for triplet O-O-O correlations in pair-additive, rigid-body models of water show a strong resemblance to the mW water model studied here, suggesting that our results are relevant for experimental systems [49].

In this Letter, we have shown that there are both qualitative and quantitative differences between tetrahedral and simple liquids in structural reorganization and associated thermodynamic signatures preceding crystallization. Using the multiparticle correlation expansion of the fluid entropy, it is established that enhanced triplet correlations and the heat capacity anomaly of tetrahedral liquids are directly related. The implications for supercooling and crystallization kinetics of several important tetrahedral liquids, such as water, silicon, germanium, and silica, are significant and can be experimentally investigated using x-ray or neutron scattering. Triplet correlations are expected to be important in various colloidal fluids that self-assemble to form low-density, ordered structures, such as diamond lattices [12,50–53]. Experimental tools such as confocal video microscopy can be used to directly compute triplet correlation functions for colloidal fluids from which entropic changes associated with self-assembly can be obtained. While this study focuses on the connections between structural correlations and excess entropy, the implications of enhancing triplet correlations for dynamics can be explored using mode-coupling theory [54] or excess entropy scaling

of dynamical properties [10,55]. The results of this study should therefore be of relevance to experimentalists and theoreticians working on simple and complex fluids, soft materials, and self-assembly of colloids and nanoparticles.

This work was financially supported by the Department of Science and Technology, New Delhi (C.C.) and the National Science Foundation through Grant No. CHE-1012651 (V. M. and A. N. H.). Computational resources from the Computer Services Centre of Indian Institute of Technology Delhi and the Centre for High Performance Computing, University of Utah are acknowledged. M. S. and D. D. thank the University Grants Commission for support through Senior and Junior Research Fellowships, respectively.

*Corresponding author.
charus@chemistry.iitd.ac.in

[1] J.-L. Barrat and J.-P. Hansen, *Basic Concepts for Simple and Complex Liquids* (Cambridge University Press, Cambridge, England, 2003).
[2] J.-P. Hansen and I. R. McDonald, *Theory of Simple Liquids* (Elsevier, New York, 2006).
[3] T. S. Ingebrigtsen, T. B. Schrøder, and J. C. Dyre, Phys. Rev. X **2**, 011011 (2012).
[4] C. A. Angell, R. D. Bressel, M. Hemmati, E. J. Sare, and J. C. Tucker, Phys. Chem. Chem. Phys. **2**, 1559 (2000).
[5] F. H. Stillinger and T. A. Weber, Phys. Rev. B **31**, 5262 (1985).
[6] P. G. Debenedetti, J. Phys. Condens. Mater. **15**, R1669 (2003).
[7] J. R. Errington and P. G. Debenedetti, Nature (London) **409**, 318 (2001).
[8] R. Sharma, S. N. Chakraborty, and C. Chakravarty, J. Chem. Phys. **125**, 204501 (2006).
[9] B. S. Jabes, M. Agarwal, and C. Chakravarty, J. Chem. Phys. **132**, 234507 (2010).
[10] D. Nayar and C. Chakravarty, Phys. Chem. Chem. Phys. **15**, 14162 (2013).
[11] I. Saika-Voivod, F. Romano, and F. Sciortino, J. Chem. Phys. **135**, 124506 (2011).
[12] Y. Wang, Y. Wang, D. R. Breed, V. N. Manoharan, L. Feng, A. D. Hollingsworth, M. Weck, and D. J. Pine, Nature (London) **491**, 51 (2012).
[13] M. Wilson, Phys. Chem. Chem. Phys. **14**, 12701 (2012).
[14] R. M. Lynden-Bell and P. G. Debenedetti, J. Phys. Chem. B **109**, 6527 (2005).
[15] V. Molinero, S. Sastry, and C. A. Angell, Phys. Rev. Lett. **97**, 075701 (2006).
[16] M. H. Bhat, V. Molinero, E. Soignard, V. C. Solomon, S. Sastry, J. L. Yarger, and C. A. Angell, Nature (London) **448**, 787 (2007).
[17] V. Molinero and E. B. Moore, J. Phys. Chem. B **113**, 4008 (2009).
[18] W. Hujo, B. S. Jabes, V. K. Rana, C. Chakravarty, and V. Molinero, J. Stat. Phys. **145**, 293 (2011).
[19] H. S. Green, *The Molecular Theory of Fluids* (North-Holland Pub. Co., Amsterdam, 1952).
[20] R. D. Mountain and H. J. Raveché, J. Chem. Phys. **55**, 2250 (1971).
[21] D. C. Wallace, J. Chem. Phys. **87**, 2282 (1987).
[22] A. Baranyai and D. J. Evans, Phys. Rev. A **40**, 3817 (1989).
[23] A. Baranyai and D. J. Evans, Phys. Rev. A **42**, 849 (1990).
[24] T. Arisawa, T. Arai, and I. Yokoyama, Physica (Amsterdam) **262B**, 190 (1999).
[25] E. B. Moore and V. Molinero, J. Chem. Phys. **130**, 244505 (2009).
[26] D. Limmer and D. Chandler, J. Chem. Phys. **135**, 134503 (2011).
[27] D. T. Limmer and D. Chandler, J. Chem. Phys. **138**, 214504 (2013).
[28] V. V. Vasisht, S. Saw, and S. Sastry, Nat. Phys. **7**, 549 (2011).
[29] T. Li, D. Donadio, G. Russo, and G. Galli, Phys. Chem. Chem. Phys. **13**, 19807 (2011).
[30] A. Reinhardt and J. P. K. Doye, J. Chem. Phys. **136**, 054501 (2012).
[31] H. J. Raveché, J. Chem. Phys. **55**, 2242 (1971).
[32] B. B. Laird and A. D. J. Haymet, Phys. Rev. A **45**, 5680 (1992).
[33] J. A. Krumhansl and S.-S. Wang, J. Chem. Phys. **56**, 2034 (1972).
[34] W. J. McNeil, W. G. Madden, A. D. J. Haymet, and S. A. Rice, J. Chem. Phys. **78**, 388 (1983).
[35] G. Hummer, A. E. Garcia, and D. M. Soumpasis, Faraday Discuss. **103**, 175 (1996).
[36] See Supplemental Material at http://link.aps.org/supplemental/10.1103/PhysRevLett.112.147801 for computational details, including molecular dynamics simulations and estimation of thermodynamic and triplet entropy.
[37] R. Agrawal and D. A. Kofke, Mol. Phys. **85**, 43 (1995).
[38] E. B. Moore and V. Molinero, Nature (London) **479**, 506 (2011).
[39] V. Holten, D. T. Limner, V. Molinero, and M. A. Anisimov, J. Chem. Phys. **138**, 174501 (2013).
[40] Y. Rosenfeld and P. Tarazona, Mol. Phys. **95**, 141 (1998).
[41] Y. Rosenfeld, Phys. Rev. E **62**, 7524 (2000).
[42] C. Chakravarty, P. G. Debenedetti, and F. H. Stillinger, J. Chem. Phys. **126**, 204508 (2007).
[43] S. N. Chakraborty and C. Chakravarty, Phys. Rev. E **76**, 011201 (2007).
[44] M. Singh, M. Agarwal, D. Dhabal, and C. Chakravarty, J. Chem. Phys. **137**, 024508 (2012).
[45] N. Gnan, T. B. Schrøder, U. R. Pedersen, N. P. Bailey, and J. C. Dyre, J. Chem. Phys. **131**, 234504 (2009).
[46] J. C. Dyre, Phys. Rev. E **87**, 022106 (2013).
[47] H. Tanaka, Eur. Phys. J. E **35**, 113 (2012).
[48] P. A. Egelstaff, D. I. Page, and C. R. T. Heard, J. Phys. C **4**, 1453 (1971).
[49] D. Nayar and C. Chakravarty, "Structural Order and the Density Anomaly in Tetrahedral Liquids" (unpublished).
[50] É. Marcotte, F. H. Stillinger, and S. Torquato, J. Chem. Phys. **138**, 061101 (2013).
[51] A. M. Kalsin, M. Fialkowski, M. Paszewski, S. K. Smoukov, K. J. M. Bishop, and B. A. Grzybowski, Science **312**, 420 (2006).
[52] K. J. M. Bishop, N. R. Chevalier, and B. A. Grzybowski, J. Phys. Chem. Lett. **4**, 1507 (2013).
[53] X. Mao, Q. Chen, and S. Granick, Nat. Mater. **12**, 217 (2013).
[54] F. Sciortino and W. Kob, Phys. Rev. Lett. **86**, 648 (2001).
[55] S. Sengupta, V. V. Vasisht, and S. Sastry, J. Chem. Phys. **140**, 044503 (2014).